IET 4th Hybrid and Electric Vehicles Conference 2013 (HEVC13),
6-8 November 2013, London. pp1-6

Comparative analysis of forward-facing models vs backward-facing models in powertrain component sizing

G Mohan, F Assadian, S Longo

Department of Automotive Engineering, Cranfield University, United Kingdom
Email: ganesh.mohan@cranfield.ac.uk

Keywords: Powertrain sizing, backward-facing model.

Abstract

Powertrain size optimisation based on vehicle class and usage profile is advantageous for reducing emissions. Backward-facing powertrain models, which incorporate scalable powertrain components, have often been used for this purpose. However, due to their quasi-static nature, backward-facing models give very limited information about the limits of the system and drivability of the vehicle. This makes it difficult for control system development and implementation in hardware-in-the-loop (HIL) test systems. This paper investigates the viability of using forward-facing models in the context of powertrain component sizing optimisation. The vehicle model used in this investigation features a conventional powertrain with an internal combustion engine, clutch, manual transmission, and final drive. Simulations that were carried out have indicated that there is minimal effect on the optimal cost with regards to variations in the driver model sensitivity. This opens up the possibility of using forward-facing models for the purpose of powertrain component sizing.

1 Introduction

Optimising powertrain component size for desired vehicle class and usage profile is beneficial for reducing tail pipe emissions [1]. Backward-facing models, containing scalable powertrain components, are often used for this purpose [2, 3]. Backward-facing models do not require a driver model, and the vehicle speed trace is obtained from a given drivecycle. The speed trace is then imposed onto the vehicle model, to calculate the angular velocity and torque at the wheels. Subsequently, the angular velocity and torque at the Internal Combustion Engine (ICE) is determined "backwards" through each drivetrain component via efficiency models or maps. The efficiency maps are obtained from steady-state testing of real components, hence this is why backward-facing models are also considered as "quasi-static" models. These models also run with a relatively larger time step when compared to forward-facing models [3], resulting in quicker simulation times. These attributes have enabled backward-facing models to be used extensively in the area of powertrain component size optimisation [4, 5].

However, because of their quasi-static nature, backward-facing models give very limited information about drivability of the vehicle [4]. Backward-facing models also make it difficult for control system development and implementation in hardware-in-the-loop (HIL) test systems.

Alternatively, forward-facing models feature a driver model, and it gives insight to the drivability of the vehicle. Whilst it is acknowledged that forward-facing models provide better understanding of the dynamics and physical limits of the powertrain [3, 6], there have been very little research in the area of utilising forward-facing models for the purpose of powertrain component sizing optimisation. With the potential advantages of forward-facing models over backward-facing models, this paper aims to investigate this area.

To achieve this, both backward-facing and forward-facing models are coupled with an optimiser to minimise the vehicle's fuel consumption. Sections 2 and 3 introduce the forward-facing and backward-facing models respectively. Section 4 describes the methodology, along with development of the vehicle model, the driver model, and the drivecycles used in the optimisation routine. This is followed by Section 5 with the simulations results and Section 6 with discussions. Section 7 then concludes the findings of this paper. Although a conventional powertrain is used as a case study, the methods and modelling approaches used in this paper can be applied to different types of powertrains including those in electric vehicles and hybrid electric vehicles.

2 Forward-facing model

Forward-facing models represent dynamic models with the correct causality. A forward-facing vehicle model features a driver model, which provides torque demand in the form of desired ICE torque and brake torque (positive and negative torque), to meet the speed trace from a drivecycle. The topology of the forward-facing model used in this investigation is shown in Figure 1. A basic driver model typically uses one or more Proportional-Integral (PI) controllers to achieve the torque demand, with reference to the desired speed trace. This is discussed further in the next section. The torque produced by the ICE propagates through the transmission and final drive ratios, before ending up as torque applied at the wheels. This is then exerted to the vehicle mass via force on the tyre contact patch. The vehicle speed that results from the applied force is propagated back through the drivetrain, and returns to the ICE as angular velocity at the crankshaft. Brake torque is applied directly at the wheels.

Unlike backward-facing models (Figure 2), the speed trace is not "imposed" onto the vehicle model in forward-facing models, and therefore there will inevitably be a small margin of error between the actual vehicle speed and the speed trace. It is the role of the driver model to minimise this margin of error. This is similar to the role of a real-world test driver carrying out an emissions test for vehicle type-approval.

Forward-facing models provide insight into the vehicle model drivability, and it captures the limits of the physical system. It also makes control development and implementation on HIL systems easier. However, with the presence of multiple state equations in a typical forward-facing model, vehicle speed (and subsequently drivetrain angular velocity) is computed via multiple state integration, resulting in the need to run the simulation in smaller time steps. This results longer simulation times when compared to backward-facing model.

Furthermore, resizing the powertrain will alter the dynamics of the system, potentially requiring the driver model to be re-tuned to maximise the performance of the system. This will also be one of the areas investigated in this paper.

3 Backward-facing Model

The ability of the vehicle model to meet the demands of the drivecycle is the principle assumption of a backward-facing model [3]. Based on the speed trace, the resultant force at the tyre contact patch is calculated, where it is converted into wheel torque and propagated back to the ICE via the drivetrain, along with angular velocity. As a result, there is no driver model present. With both speed and torque imposed onto the powertrain components, a backward-facing model can also be considered as acausal.

During the optimisation routine, the powertrain component sizing is determined by the ability of the component to address both the speed and torque imposed on the component (i.e. the power requirements).

Backward-facing models rely on efficiency maps that were created based on torque and speed data, and usually produced during steady-state real world testing. This results in the calculation being relatively simpler than forward-facing models (essentially lookup tables instead of state equations), and can therefore be run over relatively larger time steps.

Unfortunately, the very nature of using steady state maps hinders the performance of backward-facing models when it comes to representing dynamic effects. The acausal nature also means that backward-facing models are difficult for control system development and implementation in HIL systems.

4 Model Development

The vehicle model used in this investigation features a conventional powertrain that is found on majority of the vehicles on the road. It contains an ICE, clutch, manual transmission, and final drive. It also includes environment losses such as aerodynamic drag and rolling resistance. The ICE displacement and final drive ratio is scalable, and used as decision variables by the optimiser to minimise the cost function.

The forward-facing vehicle model is shown in Figure 1. A backward-facing model is also created as a benchmark against the forward-facing model. The backward-facing model is shown in Figure 2.

Based on Figure 1, it is observed that the transfer of power information is bi-directional in the forward-facing model, i.e. the direction of effort (torque) is opposite to the direction of flow (speed). The driver block in the forward-facing model is also absent in the backward-facing model.

In the backward-facing model, power information is mono-directional (effort and flow are in the same direction).

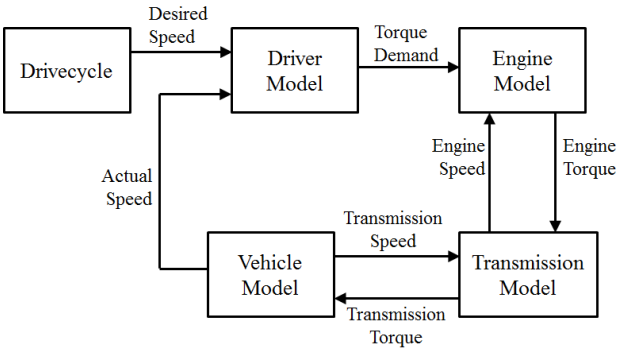

Figure 1: Forward-facing vehicle model

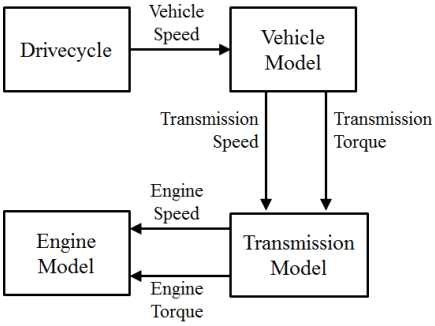

Figure 2: Backward-facing vehicle model

4.1 Vehicle Model

Both forward-facing and backward-facing models include the following parameters:

- Scalable ICE model
- Vehicle mass information (to calculate inertial load)
- Identical transmission ratios.

The following environmental forces are also imposed on both models:

- Aerodynamic drag
- Tyre rolling resistance.

4.2 Scalable ICE model

The aim of the ICE model is to be scalable and sufficiently capture the operation and efficiency envelopes of an ICE. This model is based on the Willan's line ICE model, as proposed by Guzzella [7] and Rizzoni [2], and modelled by Shankar, et al [8]. Validations of the models were carried out by Shankar, et al [9] and Wu, et al [10].

In this paper, a baseline ICE model that is naturally aspirated and spark ignited was selected, which is widely available on the market today [11, 12].

4.3 Driver Model

For the forward-facing model, two PI controllers were used in the driver model. A common integrator was shared between the two controllers, and the integrator was reset when there was a change in the sign of the error (from positive to negative or vice-versa), as a form of basic anti-windup. This implementation is shown in Figure 3.

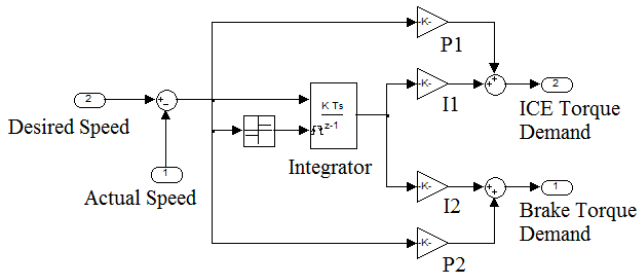

Figure 3: Driver model with two PI controllers

The two PI controllers were used to modulate positive torque (ICE) and negative torque (friction brakes) respectively. The two sets of P and I values, along with the ICE displacement and final drive ratio, form the six decision variables that are manipulated by the optimiser to minimise the cost function.

4.4 Drivecycles

Three types of drivecycles were used to evaluate the sizing of the powertrain to minimise the cost function:

- New European Drive Cycle (NEDC) [13]
- Real-world cycle [1]
- Artemis cycle [14].

The real-world cycle is shown in Figure A 1 in the Appendix, and it was derived from series of real-world usage studies undertaken by Cranfield University [1]. It combines speed traces from usage in urban, A-road, B-road and motorway sections.

4.5 Methodology

The optimisation routine can be represented in a standard form [15, 16]. Given a set of decision variables, X, and a cost function, ϕ, the optimiser aims find X_{min} to minimise ϕ, within bounds of G, where G represents the design constraints.

To optimise the vehicle for the lowest amount of fuel consumed to complete a drivecycle, the cost function *(ϕ)*, decision variables *(X)*, and constraints *(G)* are shown in Table 1.

The drivecycle speed deviation is used for the forward model only, and it is calculated as the root mean square (RMS) error between the vehicle speed trace and target drivecycle speed trace.

Term	Definition	Units
ϕ	Fuel consumed (FC)	kg
X	ICE displacement	litre
	Final drive ratio (FD ratio)	-
	P and I values (for forward-facing model)	-
G	1.0 < ICE displacement < 5.0	litre
	1 < FD ratio < 10	-
	0 < Drivecycle speed deviation < 1	kph

Table 1: Terms used for Simulations 1 and 2

The P and I values are mapped out as follows:

- P_1 is the accelerator pedal gain
- I_1 is the accelerator pedal integral
- P_2 is the brake pedal gain
- I_2 is the brake pedal integral.

5 Results

5.1 Simulation 1

Purpose of Simulation 1 was to identify the combined effect of optimising the powertrain size and driver model. It also allowed the forward-facing model to be benchmarked against the backward-facing model in terms of component sizing and minimisation of the cost function. A fixed vehicle glider mass of 1000kg was used to simulate a typical E-segment family saloon [17]. The glider mass is defined as the total mass of the vehicle minus the mass of the powertrain. The results of this simulation are shown in Figure 4 and Figure 5.

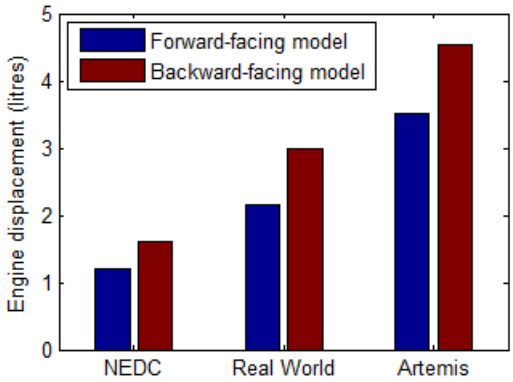

Figure 4: Optimisation of engine displacement for minimum fuel consumption for a given drivecycle

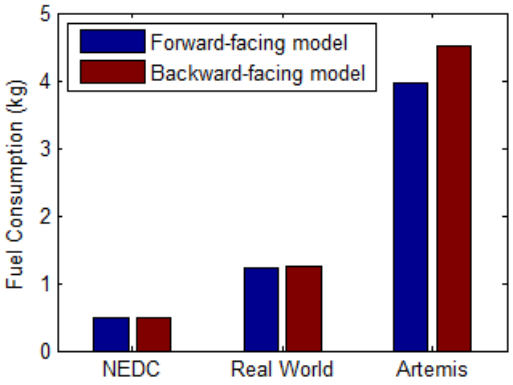

Figure 5: Resultant fuel consumed for each drivecycle

In Figure 4, the optimised engine displacement for each drivecycle is shown. In Table 2, the optimised P and I values for the driver model are shown. It is noteworthy that the values vary greatly from one drivecycle to another, and there is no observable trend.

	P_1	I_1	P_2	I_2
NEDC	82.70	3.74	328.57	9.83
Real World	48.48	0.40	492.38	9.62
Artemis	67.08	4.41	480.35	0.26

Table 2: Simulation 1 results, forward-facing model

Time taken to complete optimisation (forward-facing model):

- NEDC: 35.2 minutes
- Cranfield: 50.8 minutes
- Artemis: 95.5 minutes.

Time taken to complete optimisation (backward-facing model):

- NEDC: 2.5 minutes
- Cranfield: 4.2 minutes
- Artemis: 7.1 minutes.

5.2 Simulation 2

In Simulation 2, only the P and I values were optimised for a given drivecycle and fixed ICE displacements. The cost function is the same as Simulation 1.

The purpose of this simulation is to observe the sensitivity of the cost function towards variations in the P and I values. The simulation was carried out using forward-facing models only and for different sets of drivecycles and ICE displacements.

Three vehicle types, as shown in Table 3, were used as a case study.

	ICE displacement (litres)	Vehicle mass (kg)
Vehicle 1	1.5	1000
Vehicle 2	3.0	1500
Vehicle 3	5.0	2000

Table 3: Three vehicle types used in Simulation 2

The results in Table 4 show the results of the P and I values for each type of vehicle. The P and I values combines the results from all three drivecycles, and are represented as the standard deviation (Std Dev) and mean values respectively. The full set of results is shown in Table A 1 in the Appendix.

Vehicle 1				
	P_1	I_1	P_2	I_2
Std Dev	1.52	5.30	205.13	1.35
Mean	10.75	3.12	235.93	1.52
Vehicle 2				
Std Dev	16.23	4.46	78.33	2.73
Mean	18.56	5.30	147.51	2.00
Vehicle 3				
Std Dev	7.42	5.51	106.67	5.47
Mean	26.04	3.50	209.72	3.64

Table 4: Results of P and I values for each vehicle type

By taking the average of the mean P and I values for each vehicle type, the "global mean" was then calculated, as shown in Table 5.

Global Mean	**P_1**	**I_1**	**P_2**	**I_2**
	18.45	**3.97**	**197.72**	**2.39**

Table 5: Global mean for the P and I values

To study the sensitivity of the cost function towards variations in the P and I values, the simulation was re-run and the global mean P and I values were imposed on all vehicle types and drivecycles. The result can be seen in Figure 6, where "Optimised" refers to the fuel consumption of the vehicle using the respective optimised P and I values and "Global Mean" refers to the fuel consumption of the vehicle using the "global mean" P and I values.

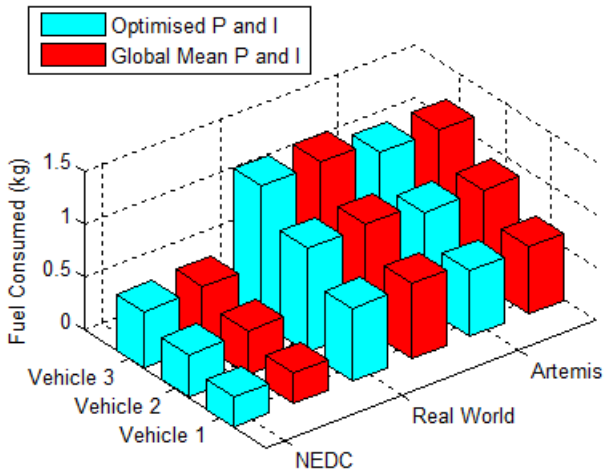

Figure 6: Sensitivity of P and I values towards the fuel consumption for each vehicle type and drivecycle

6 Discussion

Referring to the results from Simulation 1, it is noteworthy that the optimised component sizes were similar for a given drivecycle. The component sizes between the forward-facing and backward-facing models were closer for NEDC, but further away for Artemis. This could be attributed to the NEDC being less transient than the Artemis drivecycle in terms of acceleration levels. Hence, the "quasi-static" nature of the backward-facing model is not penalised as heavily in the NEDC as it is in the Artemis cycle.

In Simulation 2, it is observed that there is minimal effect on the cost function with regards to variations in the P and I values. This result opens up the possibility of using forward-facing models (with co-optimisation of the driver model) for the purpose component size optimisation. The advantages of forward-facing models, as discussed previously, is the insight that it will provide regarding the drivability of the vehicle, along with easier integration of the vehicle model in a HIL environment.

However, the simulation times of backward-facing models were also observed to be was an order of magnitude faster than the respective forward-facing models.

7 Conclusion

This investigation has given some insight into the possibility of using forward-facing models for the purpose of powertrain size optimisation. Results have suggested that this is possible when the driver model is also co-optimised along with the powertrain components.

The additional simulation time overhead imposed by forward-facing models will also be reduced over time with ever-increasing computing power. Therefore, the prospect of using forward-facing models for the purpose of powertrain component sizing is indeed achievable.

Acknowledgements

The authors wish to thank EPSRC (Grant number EP/I038586/1) and the FUTURE Vehicle consortium for their support in conducting this research.

References

[1] R. Shankar, J. Marco and S. Carroll, "Performance of an EV during real-world usage", *Cenex Hybrid Electric Vehicle Conference, UK*. 2011.

[2] G. Rizzoni, L. Guzzella and B. M. Baumann, "Unified modeling of hybrid electric vehicle drivetrains," *Mechatronics, IEEE/ASME Transactions on,* vol. 4, pp. 246-257, 1999.

[3] K. B. Wipke, M. R. Cuddy and S. D. Burch, "ADVISOR 2.1: a user-friendly advanced powertrain simulation using a combined backward/forward approach," *Vehicular Technology, IEEE Transactions on,* vol. 48, pp. 1751-1761, 1999.

[4] D. W. Gao, C. Mi and A. Emadi, "Modeling and Simulation of Electric and Hybrid Vehicles," *Proceedings of the IEEE,* vol. 95, pp. 729-745, 2007.

[5] T. Hofman, M. Steinbuch, R. van Druten and A. Serrarens, "Design of CVT-based hybrid passenger cars," *Vehicular Technology, IEEE Transactions on,* vol. 58, pp. 572-587, 2009.

[6] W. Xiong, Y. Zhang and C. Yin, "Optimal energy management for a series–parallel hybrid electric bus," *Energy Conversion and Management,* vol. 50, pp. 1730-1738, 2009.

[7] L. Guzzella and A. Sciarretta, *Vehicle Propulsion Systems: Introduction to Modeling and Optimization.* Springer, 2005.

[8] R. Shankar, J. Marco and F. Assadian, "The Novel Application of Optimization and Charge Blended Energy Management Control for Component Downsizing within a Plug-in Hybrid Electric Vehicle," *Energies,* vol. 5, pp. 4892-4923, 2012.

[9] R. Shankar, J. Marco and F. Assadian, "A methodology to determine drivetrain efficiency based on external environment," in *Electric Vehicle Conference (IEVC), 2012 IEEE International,* 2012, pp. 1-6.

[10] X. Wu, B. Cao, X. Li, J. Xu and X. Ren, "Component sizing optimization of plug-in hybrid electric vehicles," *Appl. Energy,* vol. 88, pp. 799-804, 2011.

[11] A. Bandivadekar, *On the Road in 2035: Reducing Transportation's Petroleum Consumption and GHG Emissions.* Massachusetts Institute of Technology, 2008.

[12] M. Contestabile, G. J. Offer, R. Slade, F. Jaeger and M. Thoennes, "Battery electric vehicles, hydrogen fuel cells and biofuels. Which will be the winner?" *Energy Environ. Sci.,* vol. 4, pp. 3754-3772, 2011.

[13] T. Barlow, S. Latham, I. McCrae and P. Boulter, *A Reference Book of Driving Cycles for use in the Measurement of Road Vehicle Emissions.* 2009.

[14] M. André, R. Joumard, R. Vidon, P. Tassel and P. Perret, "Real-world European driving cycles, for measuring pollutant emissions from high-and low-powered cars," *Atmos. Environ.,* vol. 40, pp. 5944-5953, 2006.

[15] R. J. Balling and J. Sobieszczanski-Sobieski, *Optimization of Coupled Systems: A Critical Overview of Approaches.,* 1994.

[16] S. Kodiyalam and J. Sobieszczanski-Sobieski, "Multidisciplinary design optimisation-some formal methods, framework requirements, and application to vehicle design," *Int. J. Veh. Des.,* vol. 25, pp. 3-22, 2001.

[17] A. S. A. Ferreira Pinto, "Evolution of weight, fuel consumption and CO_2," 2009.

Appendix

Vehicle 1				
	P_1	I_1	P_2	I_2
NEDC	11.05	0.03	470.43	0.60
Real World	12.09	0.08	147.61	3.07
Artemis	9.11	9.24	89.76	0.89
Std Dev	**1.52**	**5.30**	**205.13**	**1.35**
Mean	**10.75**	**3.12**	**235.93**	**1.52**
Vehicle 2				
NEDC	8.97	0.43	171.42	0.19
Real World	37.30	9.20	60.01	0.67
Artemis	9.40	6.27	211.09	5.15
Std Dev	**16.23**	**4.46**	**78.33**	**2.73**
Mean	**18.56**	**5.30**	**147.51**	**2.00**
Vehicle 3				
NEDC	20.26	0.07	265.76	0.72
Real World	34.41	9.85	86.71	0.25
Artemis	23.44	0.58	276.70	9.95
Std Dev	**7.42**	**5.51**	**106.67**	**5.47**
Mean	**26.04**	**3.50**	**209.72**	**3.64**

Table A 1: Results from Simulation 2

	Vehicle 1			
	Fuel Optimised (kg)	Fuel Global Mean (kg)	Speed Dev Optimised (kph)	Speed Dev Gbl Mean (kph)
NEDC	0.28	0.29	1.53	0.60
Real World	0.69	0.71	1.68	0.82
Artemis	0.62	0.63	2.00	1.24
	Vehicle 2			
NEDC	0.40	0.41	1.87	0.85
Real World	0.98	0.99	2.00	1.11
Artemis	0.89	0.89	1.87	1.67
	Vehicle 3			
NEDC	0.53	0.55	1.60	1.11
Real World	1.29	1.30	1.93	1.38
Artemis	1.18	1.18	1.99	2.07

Table A 2: Comparison between optimised and global P and I values

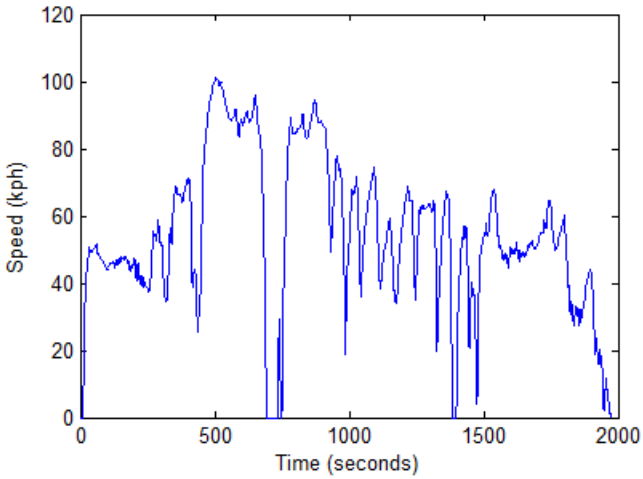

Figure A 1: The real-world drivecycle